Seismic Signal Deconvolution Using a Maximum Posterior Mode Algorithm

Idan Ram, Israel Cohen, and Shalom Raz, Technion – Israel Institute of Technology, and Anthony A. Vassiliou, GeoEnergy*

SUMMARY

In this paper we introduce a multichannel blind deconvolution algorithm for the restoration of two-dimensional (2D) seismic data. This algorithm is based on a 2D reflectivity prior model, which takes into account the spatial dependency between neighboring traces. Each reflectivity column is estimated from the corresponding observed trace using the estimate of the preceding reflectivity column and a modified maximum posterior mode (MPM) algorithm. The MPM algorithm employs a Gibbs sampler to simulate realizations of seismic reflectivities. We apply the algorithm to synthetic and real data, and demonstrate improved results compared to those obtained by a single-channel deconvolution method.

INTRODUCTION

Multichannel blind seismic deconvolution aims at restoring a two-dimensional (2D) reflectivity section and an unknown seismic pulse (wavelet) from 2D observed seismic data. Under simplifying assumptions, the seismic data can be modeled as a result of convolution between the reflectivity section and a one-dimensional (1D) seismic wavelet, degraded by additive noise.

Many methods rely on the assumption that the wavelet is a 1D vertical signal and break the multichannel deconvolution problem into independent 1D deconvolution problems. Kormylo and Mendel (1982) use second order statistics methods to estimate an autoregressive moving average wavelet and the Single Most Likely Replacement (SMLR) algorithm to recover a Bernoulli-Gaussian (BG) reflectivity. Kaaresen and Taxt (1998) estimate a finite impulse response wavelet using a least-squares fit and recover a BG reflectivity using the iterated window maximization algorithm proposed in Kaaresen (1997). Cheng et al. (1996) estimate simultaneously a Bernoulli-Gaussian reflectivity and a moving average wavelet using a Bayesian framework in which prior information is imposed on the seismic wavelet, BG reflectivity parameters and the noise variance. Rosec et al. (2003) use a moving average wavelet and model the reflectivity sequence as a mixture of Gaussian distributions (Lavielle (1995)). They propose both the stochastic expectation maximization (SEM) algorithm (Celeux and Diebolt (1985), Celeux et al. (1996)) and a Bayesian framework for parameter estimation. The estimated parameters are employed by the maximum posterior mode (MPM) algorithm (Chalmond (1989)), which uses realizations of the reflectivity simulated by a Gibbs sampler (Robert (1994), Geman and Geman (1984)) to estimate the reflectivity.

Application of 1D restoration methods to 2D seismic data is clearly suboptimal, as it does not take into account the correlation between neighboring traces, which stems from the presumed continuous and roughly horizontal structure of the earth layers. Idier and Goussard (1993) proposed a multichannel deconvolution method, which takes into account the stratification of the layers, and uses two 2D reflectivity models: Markov-Bernoulli-Gaussian (MBG) I and II. The deconvolution is carried out using a suboptimal maximum a posteriori (MAP) estimator, which iteratively recovers the columns of the reflectivity section. Each reflectivity column is estimated from the corresponding observed trace and the estimate of the previous reflectivity column, using an SMLR-type method. Kaaresen and Taxt (1998) also suggest a multichannel version of their blind deconvolution algorithm, which encourages spatial continuity of the estimated reflectors using an optimization criterion which penalizes non-sparse and non-continuous configurations. Heimer et al. (2007) and Heimer and Cohen (2008) introduced a multichannel blind deconvolution method which combines the algorithm of Kaaresen and Taxt with dynamic programming (Amini et al. (1990), Buckley and Yang (1997)) to find continuous paths of reflectors across the channels of the reflectivity section. However, layer discontinuities are not taken into account by this method. Heimer and Cohen (2009) also proposed a multichannel blind deconvolution algorithm which is based on the MBG I reflectivity model and recover the reflectivity section using the Viterbi algorithm (Forney (1973)).

In this paper, which summarizes some of the results in Ram et al. (2010), we introduce a multichannel blind deconvolution algorithm. The algorithm is based on the MBG I reflectivity model and iteratively deconvolves the seismic data, while taking into account the spatial dependency between neighboring traces. The algorithm employs in each step a modified version of the MPM algorithm which first employs a Gibbs sampler to simulate realizations of each column of the 2D reflectivity, and then estimates this column from its realizations. Experimental results on synthetic and real data demonstrate improved results compared to those obtained by the single-channel deconvolution method of Rosec et al. (2003).

REFLECTIVITY MODEL

We assume that the seismic wavelet $\mathbf{h}$ is a 1D vertical vector of length N_h, which is invariant in both horizontal and vertical directions. The reflectivity section $\mathbf{R}$ is a matrix of size $N_r \times J$ and the 2D seismic data $\mathbf{Y}$ is a matrix of size $N_y \times J$, where $N_y = N_h + N_r - 1$. $\mathbf{Y}$ can be modeled as the following noise-corrupted convolution product:

$$\mathbf{Y} = \mathbf{h} * \mathbf{R} + \mathbf{W} \tag{1}$$

where $\mathbf{W}$ is a matrix of size $N_y \times J$ which denotes an additive white Gaussian noise independent of $\mathbf{R}$ with zero mean and variance σ_w^2.

We use the MBG I reflectivity model proposed by Idier and Goussard (1993) so that the stratification of the layers of the Earth will be taken into account in the deconvolution process. This model is composed of a Markov-Bernoulli random field (MBRF), which controls the geometrical characteristics of the reflectivity, and an amplitude field, defined conditionally to the MBRF. The MBRF comprises two types of binary variables: location variables and transition variables. The location variables, set in a $N_r \times J$ matrix $\mathbf{Q}$, indicate the position of layer boundaries. Let $q_{k,j}$ denote the location variable in the (k,j) position of $\mathbf{Q}$. Then $q_{k,j}$ is set to one if a reflector exists in the (k,j) position of $\mathbf{R}$, and is set to zero otherwise. The transition variables, set in three $N_r \times J-1$ matrices $\mathbf{T}^{/}$, $\mathbf{T}^{-}$ and $\mathbf{T}^{\backslash}$, determine whether adjacent location variables belong to the same layer boundary or not. Let $t^{/}_{k,j}$, $t^{-}_{k,j}$, $t^{\backslash}_{k,j}$ denote the transition variables in the (k,j) positions of $\mathbf{T}^{/}$, $\mathbf{T}^{-}$ and $\mathbf{T}^{\backslash}$, respectively. Then $t^{/}_{k,j}$ is set to one if $q_{k,j}$ and $q_{k-1,j+1}$ belong to the same layer boundary and to zero otherwise. Similarly $t^{-}_{k,j}$ and $t^{\backslash}_{k,j}$ are set to one if $q_{k,j}$ belongs to the same layer boundary as $q_{k,j+1}$ and $q_{k+1,j+1}$, respectively, and to zero otherwise.

Let $p(\cdot)$ denote a probability distribution function. Then the MBRF has the following properties:

1. Separability property:
   $p\left(t^{/}_{k,j}, t^{-}_{k,j}, t^{\backslash}_{k,j}\right) = p\left(t^{/}_{k,j}\right) p\left(t^{-}_{k,j}\right) p\left(t^{\backslash}_{k,j}\right)$.
2. The jth columns of $\mathbf{Q}$, $\mathbf{T}^{/}$, $\mathbf{T}^{-}$ and $\mathbf{T}^{\backslash}$, denoted $\mathbf{q}_j$, $\mathbf{t}^{/}_j$, $\mathbf{t}^{-}_j$ and $\mathbf{t}^{\backslash}_j$, respectively, are white and Bernoulli distributed marginally from the rest of the field.
3. The characteristic parameters of the Bernoulli distributions are given by:
   $\lambda = p\left(q_{k,j}=1\right)$, $\mu^{/} = p\left(t^{/}_{k,j}=1\right)$,
   $\mu^{-} = p\left(t^{-}_{k,j}=1\right)$, $\mu^{\backslash} = p\left(t^{\backslash}_{k,j}=1\right)$.
4. Horizontal symmetry:
   $p\left(q_{k,j}, t^{/}_{k,j}, t^{-}_{k,j}, t^{\backslash}_{k,j}\right) = p\left(q_{k,j}, t^{/}_{k+1,j-1}, t^{-}_{k,j-1}, t^{\backslash}_{k-1,j-1}\right)$.
5. Isolated transition variables cannot be set to one:
   $p\left(t^{/}_{k,j}=0, t^{-}_{k,j}=0, t^{\backslash}_{k,j}=0 \,\middle|\, q_{k,j}=0\right) = 1$.
6. Discontinuities along layer boundaries are possible:
   $p\left(q_{k,j}=1 \,\middle|\, t^{/}_{k+1,j-1}=0, t^{-}_{k,j-1}=0, t^{\backslash}_{k-1,j-1}=0\right) = \varepsilon$.
7. λ is related to $\left\{\mu^{/}, \mu^{-}, \mu^{\backslash}, \varepsilon\right\}$ according to: $\lambda = 1 - \left(1-\mu^{/}\right)\left(1-\mu^{-}\right)\left(1-\mu^{\backslash}\right)(1-\varepsilon)$.

We now turn to the amplitude field $\mathbf{R}$. Let $\mathbf{r}_j$ denote the jth column of $\mathbf{R}$, and let $r_{k,j}$ denote the kth reflector in $\mathbf{r}_j$. Also, let $t^{/}_{k+1,j-1}$ (respectively, $t^{-}_{k,j-1}$, $t^{\backslash}_{k-1,j-1}$) be set to one, then we will further refer to the reflector $r_{k,j}$ as a successor of $r_{k+1,j-1}$ (respectively $r_{k,j-1}$, $r_{k-1,j-1}$) and symmetrically $r_{k+1,j-1}$ (respectively $r_{k,j-1}$, $r_{k-1,j-1}$) will be referred to as a predecessor of $r_{k,j}$. The correlation between $r_{k,j}$ and reflectors in previous columns depends on the local geometry of the layers and is described through $p\left(r_{k,j} \,\middle|\, q_{k,j}, \mathbf{t}_{j-1}, \mathbf{r}_{j-1}\right)$, where $\mathbf{t}_{j-1} = \left\{\mathbf{t}^{/}_{j-1}, \mathbf{t}^{-}_{j-1}, \mathbf{t}^{\backslash}_{j-1}\right\}$. These conditional probabilities can be separated into three cases:

1. If $q_{k,j}=0$ then there is no reflector at position (k,j), and $r_{k,j}=0$.
2. If $q_{k,j}=1$, and if $r_{k,j}$ is the unique successor of a unique predecessor $r_{k+dk,j-1}$ $(-1 \le dk \le 1)$ then
   $$r_{k,j} = a r_{k+dk,j-1} + w_r. \tag{2}$$
   where $a \in [0,1]$ and $w_r \sim N\left[0, \left(1-a^2\right)\sigma_r^2\right]$.
3. If $q_{k,j}=1$ and $r_{k,j}$ has no predecessor, has more than one predecessor, or is not a unique successor, then $r_{k,j}$ is sampled from the basic Gaussian distribution $N\left(0, \sigma_r^2\right)$.

We note that since the deconvolution problem is blind, the wavelet $\mathbf{h}$ and the parameters $\left(\lambda, \sigma_r, \sigma_w, a, \mu^{/}, \mu^{-}, \mu^{\backslash}, \varepsilon\right)$ are unknown. Thus, before the deconvolution is performed, we estimate them from the observed data using the SEM algorithm of Rosec et al. (2003), and from traces deconvolved using the MPM algorithm of Rosec et al.

RECURSIVE CAUSAL MULTICHANNEL BLIND DECONVOLUTION

Deconvolution Scheme

The MAP estimator of the matrices $\left\{\mathbf{T}^{/}, \mathbf{T}^{-}, \mathbf{T}^{\backslash}, \mathbf{Q}\right\}$, comprising the MBRF, and the amplitude field $\mathbf{R}$ is:

$$\left(\hat{\mathbf{T}}^{/}, \hat{\mathbf{T}}^{-}, \hat{\mathbf{T}}^{\backslash}, \hat{\mathbf{Q}}, \hat{\mathbf{R}}\right) = \underset{\mathbf{T}^{/}, \mathbf{T}^{-}, \mathbf{T}^{\backslash}, \mathbf{Q}, \mathbf{R}}{\operatorname{argmax}} p\left(\mathbf{T}^{/}, \mathbf{T}^{-}, \mathbf{T}^{\backslash}, \mathbf{Q}, \mathbf{R} \,|\, \mathbf{Y}\right). \tag{3}$$

Obtaining the exact MAP solution is very difficult because of the large dimension of the state-space of $\left\{\mathbf{T}^{/}, \mathbf{T}^{-}, \mathbf{T}^{\backslash}, \mathbf{Q}\right\}$. Here we use a suboptimal iterative maximization procedure:

$$\text{(1) First column: } (\hat{\mathbf{r}}_1, \hat{\mathbf{q}}_1) = \underset{\mathbf{r}_1, \mathbf{q}_1}{\operatorname{argmax}}\, p\left(\mathbf{r}_1, \mathbf{q}_1 \,|\, \mathbf{y}_1\right) \tag{4}$$

$$\text{(2) For } j \in [2,J]: \left(\hat{\mathbf{r}}_j, \hat{\mathbf{q}}_j, \hat{\mathbf{t}}_{j-1}\right) = \underset{\mathbf{r}_j, \mathbf{q}_j, \mathbf{t}_{j-1}}{\operatorname{argmax}}\, p\left(\mathbf{r}_j, \mathbf{q}_j, \mathbf{t}_{j-1} \,|\, \mathbf{y}_j, \hat{\mathbf{r}}_{j-1}, \hat{\mathbf{q}}_{j-1}\right) \tag{5}$$

where Markov Chain Monte Carlo (MCMC) methods are used for the optimization of its partial criteria. The first partial criterion can be optimized using the MPM algorithm presented by Rosec et al. (2003). Finding an optimal solution for the maximization problem (5) is very hard, since it requires examination of all the possible configurations of $\mathbf{q}_j, \mathbf{t}_{j-1}$, whose number ranges from 2^{N_r} to 8^{N_r}. Therefore, we apply instead a modified version of the MPM algorithm. This algorithm estimates the vectors $\mathbf{r}_j, \mathbf{q}_j, \mathbf{t}_{j-1}$ from realizations simulated by a Gibbs sampler, described next.

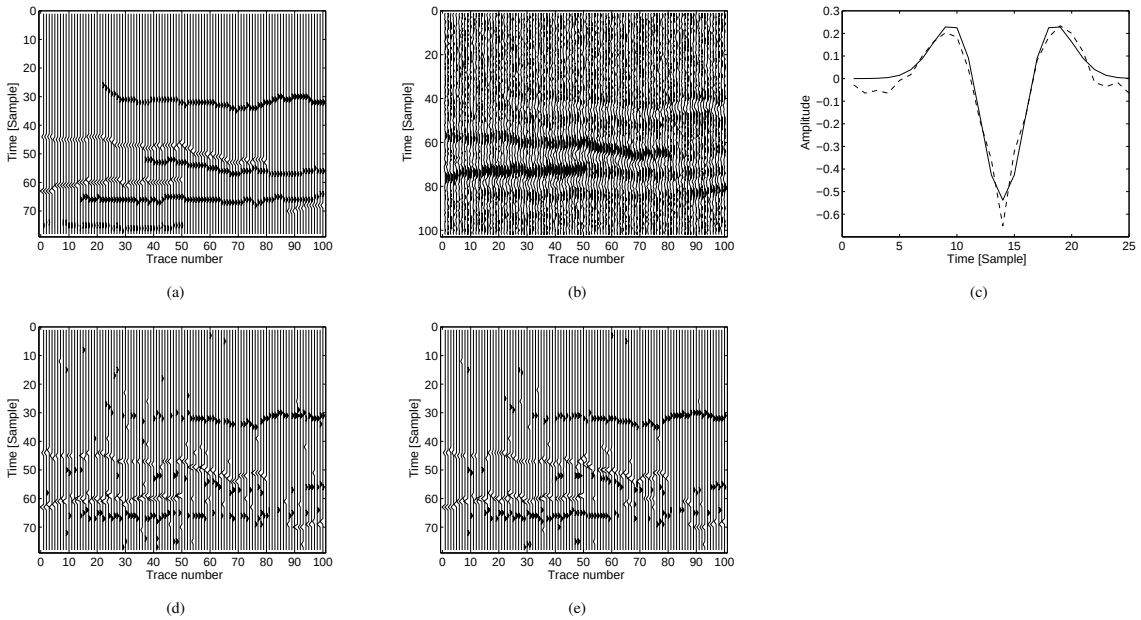

Figure 1: Synthetic 2D data deconvolution results for SNR of 0 dB: (a) Synthetic 2D reflectivity section. (b) 2D seismic data. (c) True wavelet (solid) and its estimate (dashed). (d) Single-channel deconvolution results. (e) Multichannel deconvolution results.

Gibbs Sampler

The Gibbs sampler generates samples of $\mathbf{r}_j, \mathbf{q}_j, \mathbf{t}_{j-1}$ from the joint distribution $p\left(\mathbf{r}_j, \mathbf{q}_j, \mathbf{t}_{j-1} \left| \mathbf{y}_j, \hat{\mathbf{r}}_{j-1}, \hat{\mathbf{q}}_{j-1} \right.\right)$. Instead of sampling directly from the joint distribution, the Gibbs sampler iteratively samples from the conditional distributions of $r_{k,j}, q_{k,j}, t^{/}_{k,j-1}, t^{-}_{k,j-1}$ and $t^{\backslash}_{k,j-1}$ using the following steps:

1. Initialization: choice of $\mathbf{q}_j^{(0)}$, $\mathbf{r}_j^{(0)}$ and $\mathbf{t}_{j-1}^{(0)}$.
2. For $i = 1, ..., I$
   For $k = 1, ..., N_r$
   - simulate $t^{/\,(i)}_{k,j-1} \sim B\left(\mu^{/}_{k,j-1}\right)$
   - simulate $t^{-\,(i)}_{k,j-1} \sim B\left(\mu^{-}_{k,j-1}\right)$
   - simulate $t^{\backslash\,(i)}_{k,j-1} \sim B\left(\mu^{\backslash}_{k,j-1}\right)$
   - simulate $q^{(i)}_{k,j} \sim B\left(\lambda^{b}_{k,j}\right)$
   - simulate $r^{(i)}_{k,j} \sim N\left(m^{b}_{k,j}, V^{b}_{k,j}\right)$ if $q^{(i)}_{k,j} = 1$, otherwise $r^{(i)}_{k,j} = 0$.

where $B(\alpha)$ denotes a Bernoulli distribution with parameter α, and the definitions of $\mu^{/}_{k,j-1}$, $\mu^{-}_{k,j-1}$, $\mu^{\backslash}_{k,j-1}$, $\lambda^{b}_{k,j}$, $m^{b}_{k,j}$ and $V^{b}_{k,j}$ can be found in Ram et al. (2010).

MPM algorithm

We estimate each column $\mathbf{r}_j$, $1 < j \leq J$ using a modified version of the MPM algorithm. This algorithm employs the Gibbs sampler described above, to generate realizations of $\mathbf{r}_j, \mathbf{q}_j$ and $\mathbf{t}_{j-1}$. The Gibbs sampler performs I_0 iterations until it reaches a steady state period, then the samples produced in the following iterations are used to estimate the kth samples of $\mathbf{r}_j, \mathbf{q}_j$ and $, \mathbf{t}_{j-1}$. The modified MPM algorithm follows these steps iteratively:

Table 1: Comparison Between the Quality of Restoration of the Single-Channel (SC) and Multichannel (MC) Deconvolution Algorithms, for SNR of 0 dB.

	SC	MC
$L^{miss+false}$	207.13 (13.76)	185.57 (18.01)
L^{miss}	167.94 (9.51)	148.91 (13.54)
L^{false}	145.55 (11.82)	131.9 (14.08)
L^{SSQ}	101.35 (4.46)	94.1 (6.23)
$L_2^{miss+false}$	146.65 (8.99)	123.08 (11.64)
L_2^{miss}	118.4 (5.69)	98.16 (8.46)
L_2^{false}	96.05 (8.06)	81.17 (8.93)

1. For $i = 1, ..., I$ simulate $\left(\mathbf{r}_j^{(i)}, \mathbf{q}_j^{(i)}, \mathbf{t}_{j-1}^{(i)}\right)$ using the Gibbs sampler.
2. For $k = 1, ..., N_r$
   - detection step:

$$\hat{t}^{/}_{k,j-1} = \begin{cases} 1, & \text{if } \frac{1}{I-I_0} \sum_{i=I_0+1}^{I} t^{/\,(i)}_{k,j-1} > 0.5 \\ 0, & \text{otherwise} \end{cases},$$

$$\hat{t}^{-}_{k,j-1} = \begin{cases} 1, & \text{if } \frac{1}{I-I_0} \sum_{i=I_0+1}^{I} t^{-\,(i)}_{k,j-1} > 0.5 \\ 0, & \text{otherwise} \end{cases},$$

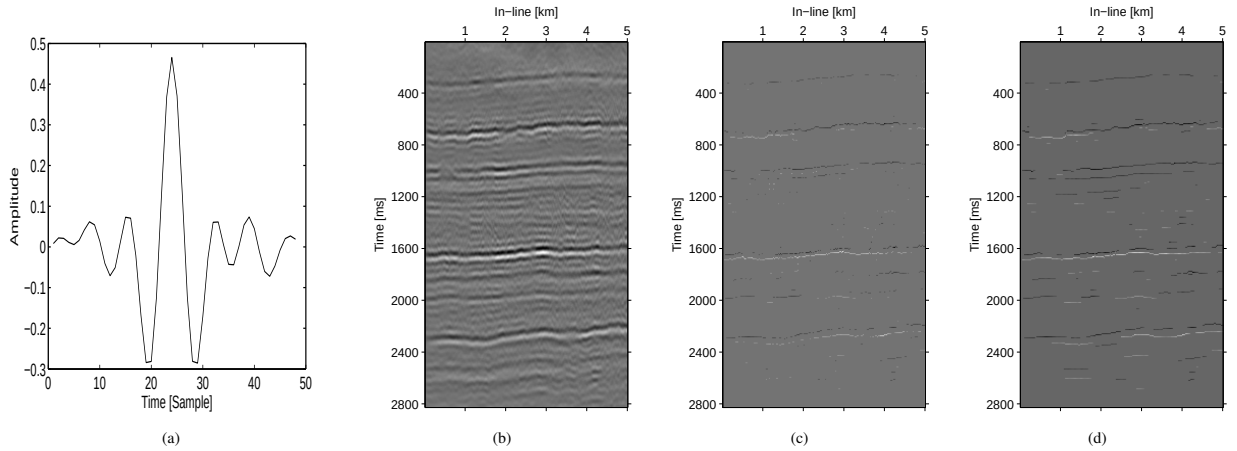

Figure 2: Real data deconvolution results: (a) Estimated wavelet. (b) Real seismic data. (c) Single-channel deconvolution results. (d) Multichannel deconvolution results.

$$\hat{t}^{\setminus}_{k,j-1} = \begin{cases} 1, & \text{if } \frac{1}{I-I_0}\sum_{i=I_0+1}^{I} t^{\setminus(i)}_{k,j-1} > 0.5 \\ 0, & \text{otherwise} \end{cases},$$

$$\hat{q}_{k,j} = \begin{cases} 1, & \text{if } \frac{1}{I-I_0}\sum_{i=I_0+1}^{I} q^{(i)}_{k,j} > 0.5 \\ 0, & \text{otherwise} \end{cases}$$

- estimation step

$$\hat{r}_{k,j} = \begin{cases} \frac{\sum_{i=I_0+1}^{I} q^{(i)}_{k,j} r^{(i)}_{k,j}}{\sum_{i=I_0+1}^{I} q^{(i)}_{k,j}(k)}, & \text{if } \hat{q}_{k,j} = 1 \\ 0, & \text{otherwise} \end{cases}$$

3. $\hat{\mathbf{r}}_j = \left[\hat{r}_{1,j},...,\hat{r}_{N_r,j}\right]^T$.

EXPERIMENTAL RESULTS

Synthetic data

We generated a 2D reflectivity section of size 76×100, shown in Fig. 1(a), using the MBG I model. We then convolved it with a 25 samples long Ricker wavelet and added white Gaussian noise, with signal to noise ratio (SNR) of 0 dB, where the SNR is defined as $SNR = 10\log_{10}\left(\frac{\lambda\sigma_r^2 E_h}{\sigma_w^2}\right)$. We created 20 such realizations, and applied to them the proposed multichannel algorithm and the single-channel MPM algorithm of Rosec et al. (2003). One such realization is shown in Figs. 1(b), and the results obtained for it by the single-channel and multichannel algorithms are depicted in Figs. 1(d) and (e), respectively. The true wavelet and the wavelet estimated for this realization are shown in Fig. 1(c). Visual comparison between these results shows improved performance of the multichannel algorithm over the performance of the single-channel algorithm. The estimates of the multichannel algorithm are more continuous, contain less false detections and are generally closer to the true reflectivity than the deconvolution results of the single-channel algorithm.

In order to quantify and compare the performances of the multichannel and single-channel algorithms, we used the four loss functions suggested in Kaaresen (1998), and three new ones defined in Ram et al. (2010). The means and standard deviations of the loss functions calculated for the estimates obtained by single-channel and multichannel deconvolution are shown in percents in Table 1. It can be seen that for all the loss functions, the multichannel algorithm achieves lower mean values than the single-channel algorithm. This implies that the multichannel algorithm produces better deconvolution results than the single-channel algorithm.

Real Data

We applied the proposed multichannel algorithm and the MPM algorithm of Rosec et al. to real seismic data from a small land 3D survey in North America (courtesy of GeoEnergy Inc., Texas) of size 400×200. The seismic data and corresponding estimated wavelet are shown in Figs. 2(b) and (a), and the reflectivity sections obtained by single-channel and multichannel deconvolution are shown in Figs. 2(c) and (d), respectively. Comparing these reflectivity sections, it can be seen that the estimates obtained by multichannel deconvolution contain layer boundaries which are more continuous and smooth than the ones obtained by the single-channel deconvolution. The multichannel algorithm also manage to detect parts of the layers that the single-channel deconvolution missed.

CONCLUSION

We have presented a multichannel blind deconvolution algorithm, which takes into account the spatial dependency between neighboring traces. Qualitative assessment of synthetic data deconvolution results shows improved performance of the proposed algorithm compared to a single-channel deconvolution algorithm.

REFERENCES

Amini, A. A., T. E. Weymouth, and R. C. Jain, 1990, Using dynamic programming for solving variational problems in vision: IEEE Transactions on Pattern Analysis and Machine Intelligence, **12**, 855–867.

Buckley, M., and J. Yang, 1997, Regularised shortest-path extraction: Pattern Recognition Letters, **18**, 621–629.

Celeux, G., D. Chauveau, and J. Diebolt, 1996, Stochastic versions of the EM algorithm: an experimental study in the mixture case: Journal of Statistical Computation and Simulation, **55**, 287–314.

Celeux, G., and J. Diebolt, 1985, The SEM algorithm: a probabilistic teacher algorithm derived from the EM algorithm for the mixture problem: Computational Statistics Quarterly, **2**, 73–82.

Chalmond, B., 1989, An iterative Gibbsian technique for reconstruction of m-ary images: Pattern Recognition, **22**, 747–761.

Cheng, Q., R. Chen, and T. H. Li, 1996, Simultaneous wavelet estimation and deconvolution of reflection seismic signals: IEEE Transactions on Geoscience and Remote Sensing, **34**, 377–384.

Forney, D. G., 1973, The Viterbi algorithm: Proceedings of the IEEE, **61**, 268–278.

Geman, S., and D. Geman, 1984, Stochastic relaxation, Gibbs distributions and the Bayesian restoration of images: IEEE Transactions on Pattern Analysis and Machine Intelligence, **6**, 721–741.

Heimer, A., and I. Cohen, 2008, Multichannel blind seismic deconvolution using dynamic programming: Signal Processing, **88**, 1839–1851.

———, 2009, Multichannel seismic deconvolution using Markov-Bernoulli random field modeling: IEEE Transactions on Geoscience and Remote Sensing, **47**, 2047–2058.

Heimer, A., I. Cohen, and A. Vassiliou, 2007, Dynamic programming for multichannel blind seismic deconvolution: Proc. Society of Exploration Geophysicist International Conference, Exposition and 77th Annual Meeting, 1845–1849.

Idier, J., and Y. Goussard, 1993, Multichannel seismic deconvolution: IEEE Transactions on Geoscience and Remote Sensing, **31**, 961–979.

Kaaresen, K. F., 1997, Deconvolution of sparse spike trains by iterated window maximization: IEEE Transactions on Signal Processing, **45**, 1173–1183.

———, 1998, Evaluation and applications of the iterated window maximization method for sparse deconvolution: IEEE Transactions on Signal Processing, **46**, 609–624.

Kaaresen, K. F., and T. Taxt, 1998, Multichannel blind deconvolution of seismic signals: Geophysics, **63**, 2093–2107.

Kormylo, J., and J. Mendel, 1982, Maximum likelihood detection and estimation of Bernoulli-Gaussian processes: IEEE Transactions on Information Theory, **28**, 482–488.

Lavielle, M., 1995, A stochastic algorithm for parametric and non-parametric estimation in the case of incomplete data: Signal Processing, **42**, 3–17.

Ram, I., C. I, and R. S, 2010, Multichannel deconvolution of seismic signals using statistical mcmc methods: to appear in IEEE Transactions on Signal Processing.

Robert, C. P., 1994, The Bayesian choice: New York: Springer-Verlag.

Rosec, O., J. Boucher, B. Nsiri, and T. Chonavel, 2003, Blind marine seismic deconvolution using statistical MCMC methods: IEEE Journal of Oceanic Engineering, **28**, 502–512.